This article was downloaded by: [University of California, San Diego]
On: 20 August 2012, At: 22:02
Publisher: Taylor & Francis
Informa Ltd Registered in England and Wales Registered Number: 1072954 Registered office: Mortimer House, 37-41 Mortimer Street, London W1T 3JH, UK

Molecular Crystals and Liquid Crystals Science and Technology. Section A. Molecular Crystals and Liquid Crystals

Publication details, including instructions for authors and subscription information:
http://www.tandfonline.com/loi/gmcl19

Influence of Longitudinal Dipole on Mesophase Formation via Computer Simulation

Katsuhiko Satoh [a] , Shigeru Mita [a] & Shoichi Kondo [a]

[a] Department of Chemistry, Faculty of Science, Science University of Tokyo, 1-3 Kagurazaka, Shinjuku-ku, Tokyo, 162, Japan

Version of record first published: 04 Oct 2006

To cite this article: Katsuhiko Satoh, Shigeru Mita & Shoichi Kondo (1997): Influence of Longitudinal Dipole on Mesophase Formation via Computer Simulation, Molecular Crystals and Liquid Crystals Science and Technology. Section A. Molecular Crystals and Liquid Crystals, 300:1, 143-161

To link to this article: http://dx.doi.org/10.1080/10587259708042344

PLEASE SCROLL DOWN FOR ARTICLE

Full terms and conditions of use: http://www.tandfonline.com/page/terms-and-conditions

This article may be used for research, teaching, and private study purposes. Any substantial or systematic reproduction, redistribution, reselling, loan, sub-licensing, systematic supply, or distribution in any form to anyone is expressly forbidden.

The publisher does not give any warranty express or implied or make any representation that the contents will be complete or accurate or up to date. The accuracy of any instructions, formulae, and drug doses should be independently verified with primary sources. The publisher shall not be liable for any loss, actions, claims, proceedings, demand, or costs or damages whatsoever or howsoever caused arising directly or indirectly in connection with or arising out of the use of this material.

Mol. Cryst. Liq. Cryst., 1997, Vol. 300, pp. 143–161
Reprints available directly from the publisher
Photocopying permitted by license only

© 1997 OPA (Overseas Publishers Association)
Amsterdam B.V. Published in The Netherlands under
license by Gordon and Breach Science Publishers
Printed in India

Downloaded by [University of California, San Diego] at 22:02 20 August 2012

Influence of Longitudinal Dipole on Mesophase Formation via Computer Simulation

KATSUHIKO SATOH, SHIGERU MITA and SHOICHI KONDO

Department of Chemistry, Faculty of Science, Science University of Tokyo, 1-3 Kagurazaka, Shinjuku-ku, Tokyo 162, Japan

(Received 22 November 1996; In final form 17 January 1997)

Monte Carlo simulations for the system composed of Gay-Berne molecules with a longitudinal dipole located near the end of the molecule have been undertaken. The system of 256 molecules of a prolate ellipsoidal shape with the dipole has been studied using the reaction field method for long-range dipolar interactions. It is found by the analysis of the microstructure that the molecules with the strong dipole form a tetragonal structure within a layer, while the nonpolar system similar to the central longitudinal dipolar system forms a hexagonal structure. The analysis of the microstructure in the nematic and isotropic phases has also been performed.

Keywords: Monte Carlo simulation; Gay-Berne potential; dipole–dipole interaction; longitudinal dipole

1. INTRODUCTION

Computer simulations have provided a useful method to understand characteristic behaviors of liquid crystals at the molecular level. Monte Carlo and molecular dynamics simulations have been performed using several models for liquid crystal molecules [1]. The realistic molecular models interacting via an atom–atom potential have been available for an analysis of structure and dynamics on substituents at the atomic level owing to recent progress of computer performance [2–4]. An investigation on dynamics and structure for the system composed of antiferroelectric liquid crystal molecules has been made using the realistic model [5].

A computer simulation using a simple model molecule is considered to be suitable for the study on the relationship between intermolecular interaction

Downloaded by [University of California, San Diego] at 22:02 20 August 2012

and the nature of liquid crystals [6–9]. It is important to determine the various conditions about density, temperature or favorable molecular shape in the simulations. Such information obtained should provide some insight into the question determining whether molecular systems exhibit liquid crystal phases or not. Two quite different approaches have been used in simulation studies of liquid crystalline systems. The first approach was due to a lattice model adopting the weak anisotropic interactions based on the Maier-Saupe mean field theory [10]. This model reproduces a nematic-isotropic phase transition, and then applications to interfacial phenomena were done [11]. Another approach employing hard bodies with an anisotropic shape was based on Onsager's theory in which the formation of liquid crystals arose from the excluded volume effect [1, 7, 8]. It is especially well known that the Gay-Berne model [12] with anisotropic repulsive and attractive terms forms various kinds of liquid crystal phases such as a nematic, a smectic A, a smectic B and a crystal phase [12–16].

The dipole is regarded to be one of the factors for controlling a fascinating feature of liquid crystals [17–19]. Therefore, the dipolar interaction in liquid crystals has been worthy of remark among a variety of interactions. It is necessary to have detailed knowledge of the effect of dipole on thermodynamical and structural properties in liquid crystals. Several theoretical studies and computer simulations have paid attention to the dipolar interaction in the formation of liquid crystals [20–24].

Monte Carlo simulations using the Gay-Berne model with a central longitudinal dipole have been reported in a previous paper [25]. In addition, the preliminary results of the system composed of molecules with the longitudinal dipole located at the terminal position in a molecule have been published about transition behavior and structure, mainly in a smectic phase [26]. In this paper we report the results of the terminal longitudinal dipolar system on the analysis of the microstructure within a layer in the smectic and crystal phases and of the microstructure of the nematic and isotropic phases in detail. Furthermore, the results are discussed in comparison with those of the central dipolar system.

2. METHOD

The total pair potential used can be expressed in the form

$$U_{\text{total}} = U_{\text{GB}} + U_{\text{Dipole}} \tag{1}$$

Downloaded by [University of California, San Diego] at 22:02 20 August 2012

where U_{GB} is the Gay-Berne potential [12],

$$U_{GB}(\hat{\mathbf{u}}_i, \hat{\mathbf{u}}_j, \mathbf{r}) = 4\varepsilon(\hat{\mathbf{u}}_i, \hat{\mathbf{u}}_j, \hat{\mathbf{r}}) \times \left[\left\{ \frac{\sigma_0}{r - \sigma(\hat{\mathbf{u}}_i, \hat{\mathbf{u}}_j, \hat{\mathbf{r}}) + \sigma_0} \right\}^{12} - \left\{ \frac{\sigma_0}{r - \sigma(\hat{\mathbf{u}}_i, \hat{\mathbf{u}}_j, \hat{\mathbf{r}}) + \sigma_0} \right\}^{6} \right] \tag{2}$$

where $\hat{\mathbf{u}}_i$ stands for the axial vector of particle i, $\hat{\mathbf{r}}$ is the unit vector of interparticle vector $\mathbf{r} = \mathbf{r}_i - \mathbf{r}_j$, and $r = |\mathbf{r}_i - \mathbf{r}_j|$ is the particle separation in which $\mathbf{r}_i$ and $\mathbf{r}_j$ are the positional vectors of the centers of particles i and j, respectively. The strength parameter $\varepsilon(\hat{\mathbf{u}}_i, \hat{\mathbf{u}}_j, \hat{\mathbf{r}})$ and the range parameter $\sigma(\hat{\mathbf{u}}_i, \hat{\mathbf{u}}_j, \hat{\mathbf{r}})$ are given by the Berne-Pechukas-Kushick function [27, 28]

$$\sigma(\hat{\mathbf{u}}_i, \hat{\mathbf{u}}_j, \hat{\mathbf{r}}) = \sigma_0 \left[1 - \frac{1}{2}\chi \left\{ \frac{(\hat{\mathbf{r}} \cdot \hat{\mathbf{u}}_i + \hat{\mathbf{r}} \cdot \hat{\mathbf{u}}_j)^2}{1 + \chi(\hat{\mathbf{u}}_i \cdot \hat{\mathbf{u}}_j)} + \frac{(\hat{\mathbf{r}} \cdot \hat{\mathbf{u}}_i - \hat{\mathbf{r}} \cdot \hat{\mathbf{u}}_j)^2}{1 - \chi(\hat{\mathbf{u}}_i \cdot \hat{\mathbf{u}}_j)} \right\} \right]^{-1/2} \tag{3}$$

$$\varepsilon(\hat{\mathbf{u}}_i, \hat{\mathbf{u}}_j, \hat{\mathbf{r}}) = \varepsilon_0 \{1 - \chi^2(\hat{\mathbf{u}}_i \cdot \hat{\mathbf{u}}_j)^2\}^{-\nu/2} \left[1 - \frac{\chi'}{2} \left\{ \frac{(\hat{\mathbf{r}} \cdot \hat{\mathbf{u}}_i + \hat{\mathbf{r}} \cdot \hat{\mathbf{u}}_j)^2}{1 + \chi'(\hat{\mathbf{u}}_i \cdot \hat{\mathbf{u}}_j)} + \frac{(\hat{\mathbf{r}} \cdot \hat{\mathbf{u}}_i - \hat{\mathbf{r}} \cdot \hat{\mathbf{u}}_j)^2}{1 - \chi'(\hat{\mathbf{u}}_i \cdot \hat{\mathbf{u}}_j)} \right\} \right]^{\mu} \tag{4}$$

where χ and χ' are the shape anisotropy and the anisotropy in the well depth parameters, respectively. These parameters are expressed as

$$\chi = \{(\sigma_e/\sigma_s)^2 - 1\}/\{(\sigma_e/\sigma_s)^2 + 1\} \tag{5}$$

$$\chi' = \{1 - (\varepsilon_e/\varepsilon_s)^{1/\mu}\}/\{1 + (\varepsilon_e/\varepsilon_s)^{1/\mu}\} \tag{6}$$

where σ_e is the separation when the molecules are positioned end-to-end and σ_s is that when they are positioned side-by-side. In other words, σ_e and σ_s essentially represent the length and breadth of the particle. The parameters ε_e and ε_s are the potential well depths for end-to-end and side-by-side configurations, respectively. We use the parameters of the axial ratio $\sigma_e/\sigma_s = 3.0$ and the well depth ratio $\varepsilon_e/\varepsilon_s = 0.2$, and the exponent parameters ($\mu = 1$, $\nu = 2$) introduced by Luckhurst *et al.* [14]. The results of the simulation for this model are given in the length and energy units of σ_0 and ε_0.

The dipole-dipole interaction is expressed as

$$U_{\text{Dipole}} = \frac{(\boldsymbol{\mu}_i \cdot \boldsymbol{\mu}_j) r^2 - 3(\boldsymbol{\mu}_i \cdot \mathbf{r})(\boldsymbol{\mu}_j \cdot \mathbf{r})}{r^5} \tag{7}$$

where μ is the longitudinal dipole moment located at a distance of $1.0\sigma_0$ from the center of a particle. The scaled intermolecular separation, $r^*(\equiv r/\sigma_0)$ is used in this paper.

Monte Carlo calculations were performed with 256 particles in a tetragonal cell as the simulation box with the usual periodic boundary conditions in the standard sampling scheme introduced by Metropolis *et al.* [29]. A series of simulations was performed in the range of 1.0 to 4.0 for the reduced temperature, $T^*(\equiv kT/\varepsilon_0)$, and in the reduced dipole moment, $\mu^*(\equiv \mu/\sqrt{\sigma_0^3\varepsilon_0})$ of 0.0, 1.0, 1.5 and 2.0, at a fixed reduced number density, $\rho^*(\equiv N\sigma_0^3/V) = 0.3$.

In all calculations, the cutoff radius, r_c, beyond which the short-range interaction potential was set at equal to zero, was taken as half the shorter length in the simulation cell ($L_{\min}/2 \approx 4.2\sigma_0$). The long-range dipolar interaction was treated by the reaction field method [30, 31] in order to facilitate the programming and to enable a more direct comparison of the results of the simulations and theories.

The additional term in the reaction field is defined as [30, 31]

$$U_{ij}^{\mathrm{RF}} = -\frac{2(\varepsilon'-1)}{2\varepsilon'+1}\frac{\mathbf{u}_i\cdot\mathbf{u}_j}{r_c^3} \qquad r_{ij} < r_c, \tag{8}$$

$$= 0 \qquad r_{ij} \geqslant r_c$$

where ε' is the dielectric constant of the continuum. In the calculations, we set $\varepsilon' = \infty$ (conducting boundary condition). In order to analyze the orientational structure, the first- and second-rank orientational order parameters, $\langle P_1\rangle$, $\langle P_2\rangle$, were calculated. The second-rank order parameter $\langle P_2\rangle$ is defined as the average of the largest eigenvalue of the tensor [32, 33],

$$Q_{\alpha\beta} = \frac{1}{N}\sum_{i=1}^{N}\frac{1}{2}(3\hat{\mathbf{u}}_{i\alpha}\hat{\mathbf{u}}_{i\beta} - \delta_{\alpha\beta}) \tag{9}$$

where $\hat{\mathbf{u}}_{i\alpha}$ is the α-component of the unit vector along the symmetry axis of particle i. The director of the system corresponds to the eigenvector. The first-rank order parameter is defined as the average of the value,

$$P_1 = \frac{1}{N}\left|\sum_{i=1}^{N}\hat{\mathbf{u}}_i\cdot\hat{\mathbf{d}}\right| \tag{10}$$

Downloaded by [University of California, San Diego] at 22:02 20 August 2012

where $\hat{\mathbf{d}}$ is the director corresponding to the eigenvector $Q_{\alpha\beta}$ mentioned above. Initial configurations were set to be an isotropic state containing randomly oriented particles, and the results of phases formed spontaneously by the cooling process were examined. In addition, we have also obtained the same results on heating starting from the perfectly aligned smectic state with a hexagonal-like structure within the layers in which the dipoles were aligned in the alternate direction.

At each temperature, the system was equilibrated in 5.0×10^5 to 3.0×10^6 moves per particle and then an additional 1.0×10^5 moves per particle were generated. Statistical errors were estimated as standard deviations from the average over these runs. The preceding configuration in a series of calculations was used for a subsequent calculation by reducing or increasing the temperature.

3. RESULTS AND DISCUSSION

The first- and second-rank orientational order parameters are shown for the system composed of molecules with a longitudinal dipole moment of $\mu^* = 2.0$ located near the end of a molecule on cooling and on heating in Figure 1. Because the same temperature dependence is exhibited in both processes except the behavior depending on the initial configurations at the lower-temperature region, the results obtained from the cooling process are reliable. In this paper, the orientational order and structural properties are hereinafter investigated in the phases formed spontaneously from an isotropic phase.

Simulations for the system established that the dipole near the end of a molecule caused a shift in the nematic-isotropic transition toward a higher temperature [26]. It is demonstrated in Figure 2 that the dipolar Gay-Berne model can qualitatively account for the behavior of the transition temperature for real compounds, for example, the phenylpyrimidine series [34, 35]. In addition, it was apparent from the longitudinal and transverse pair correlation functions that the dipole near the end of a molecule had a tendency to disturb the layer formation [26].

3.1. Isotropic and Nematic Phases

For an inspection of the dependence of the dipolar position on a short-range orientational order, Figures 3 and 4 show the dipole-dipole correlations as a function of intermolecular distance taken to be the separation

Downloaded by [University of California, San Diego] at 22:02 20 August 2012

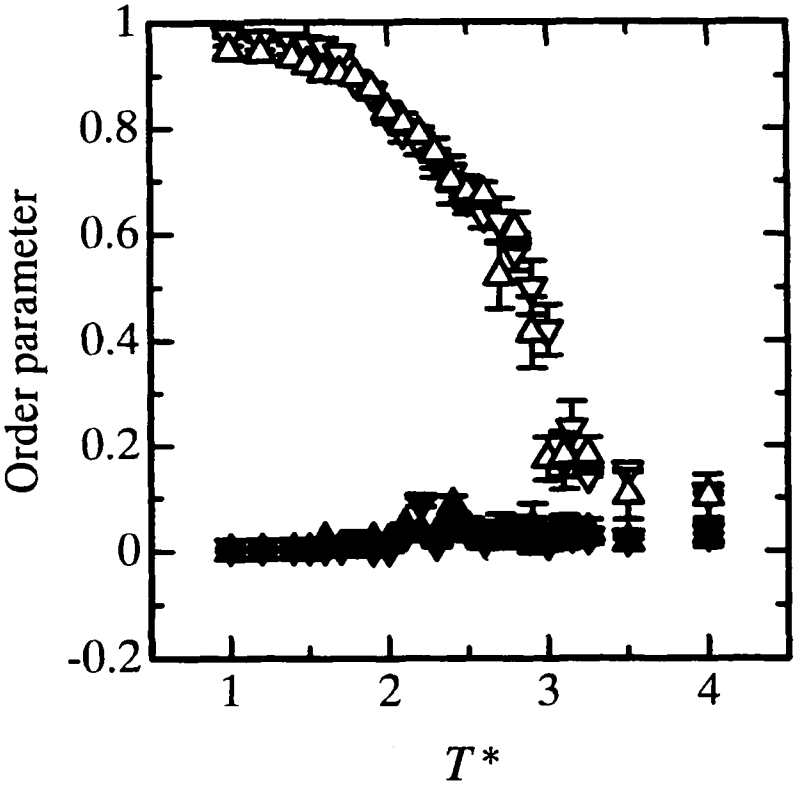

FIGURE 1 Temperature dependence of the orientational order parameters for the terminal dipolar systems for $\mu^* = 2.0$ on cooling and heating. Closed symbols denote $\langle P_1 \rangle$ values. Open symbols denote $\langle P_2 \rangle$ values. Triangles, on cooling; reverse triangles, on heating.

between the centers of mass, or between the point dipoles in the isotropic and nematic phases which were assigned in the previous [25, 26]. The correlation function is defined as

$$h(r) = 3\langle \cos \theta_{ij}(r) \rangle \tag{11}$$

where θ_{ij} is the angle between the axes of two particles separated by r. Negative and positive peaks imply correlations of antiparallel and parallel pairs, respectively.

In the isotropic phase (Fig. 3), no sign of a local order is observed for the central dipolar systems independent of the strength of the dipole moment (a), (b). However, the correlation as a function of the distance between the point dipoles for the system with a terminal dipole moment of 1.0 exhibits a

Downloaded by [University of California, San Diego] at 22:02 20 August 2012

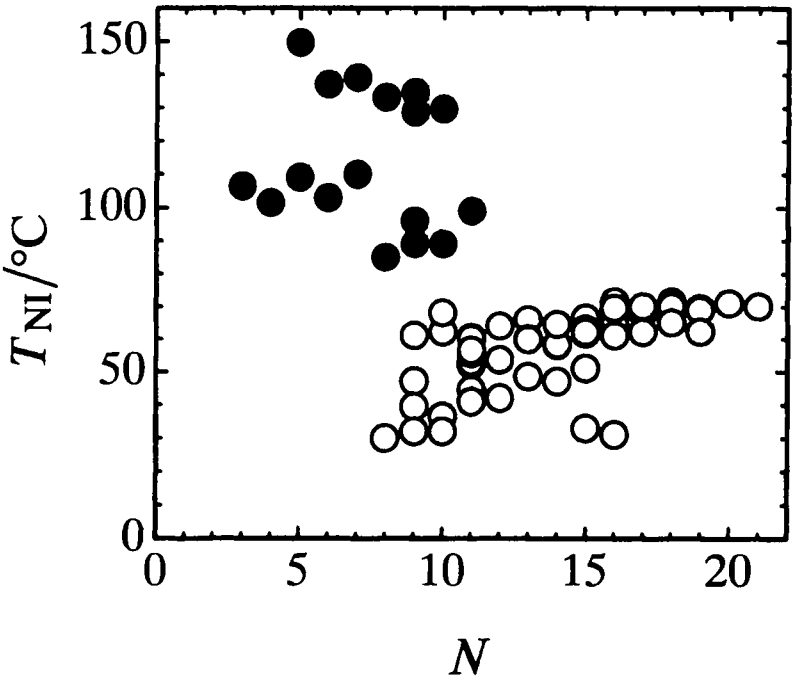

FIGURE 2 The nematic-isotropic transition temperatures for the phenylpyrimidine series as a function of the number of skeleton atoms, N in the side chains or substituent. ●, cyano substituent; ○, alkyl or alkoxy chains.

weak negative peak at a distance of *ca.*0.75 (c), and this peak for the same system with $\mu^* = 2.0$ (d) can be seen clearly. Even in the isotropic phase, there is likely to be an indication of a weak dimerization or antiparallel pair, or an orientational ordering in the short range owing to the terminal dipole for the strong polar system.

In the nematic phase (Fig. 4) exhibiting $\langle P_2 \rangle$ of *ca.*0.6, this peak is hardly seen even for the central polar system with $\mu^* = 1.0$ (a), although the peak is noticed at *ca.*1.0 for the system with $\mu^* = 2.0$ (b). On the other hand, the correlations for the terminal dipolar systems (c), (d) become intenser in comparison with those in the isotropic phase.

In order to indicate more clearly the relation between the positional and orientational orders in the isotropic and nematic phases, the center-of-mass radial distributions are shown in Figure 5. No difference was found in the distributions of all systems in the both phases. Therefore, in the case of the terminal dipole moment the short-range orientational order was found not only in the nematic phase but also in the isotropic phase, although the

Downloaded by [University of California, San Diego] at 22:02 20 August 2012

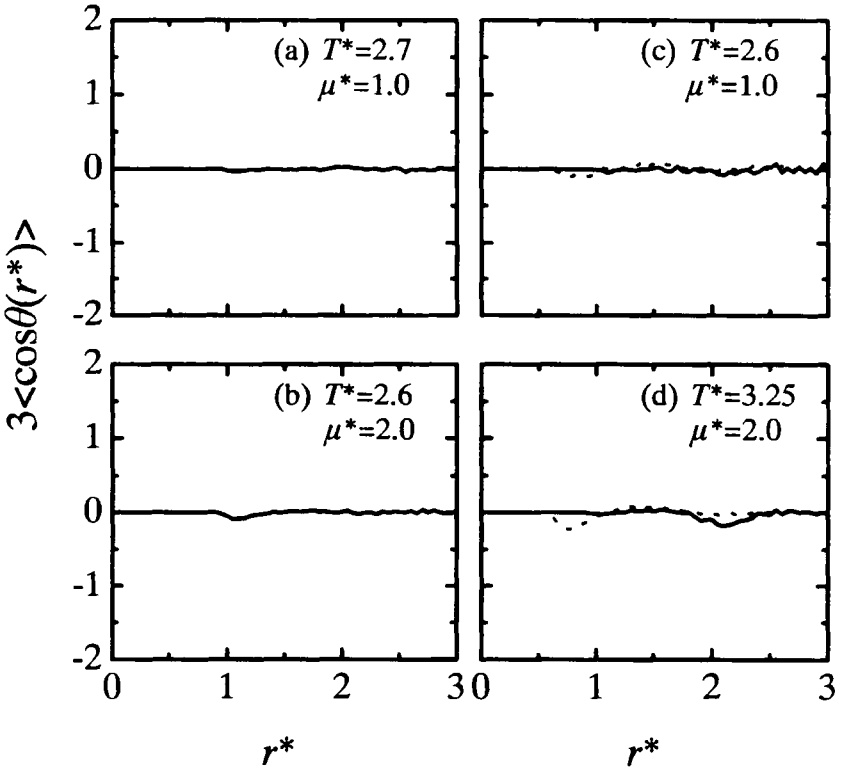

FIGURE 3 The dipole-dipole correlations as a function of intermolecular distance in the isotropic phase. Solid lines denote $3\langle\cos\theta(r)\rangle$ as a function of the separation between the centers-of-mass and dotted lines denote it as a function of the separation between the point dipoles. (a), (b) central dipolar systems; (c), (d) terminal dipolar systems.

terminal dipole has no influence on the positional order in the isotropic and nematic phases. Regardless the strength of dipole the system was not found to form a ferroelectric nematic phase as reported in a literature [21].

3.2. Smectic and Crystalline Phases

The longitudinal and transverse pair correlations for the terminal dipolar system are shown in Figure 6. The phase is assigned clearly to be the smectic phase because the periodic nature of the density wave shows a layer structure in a longitudinal correlation and the periodicity in a transverse correlation is absent. The phase assignments for the central dipolar system were already done in a previous [25]. Figure 7 shows the dipole-dipole correlation functions in the smectic phase in the case of almost the same

Downloaded by [University of California, San Diego] at 22:02 20 August 2012

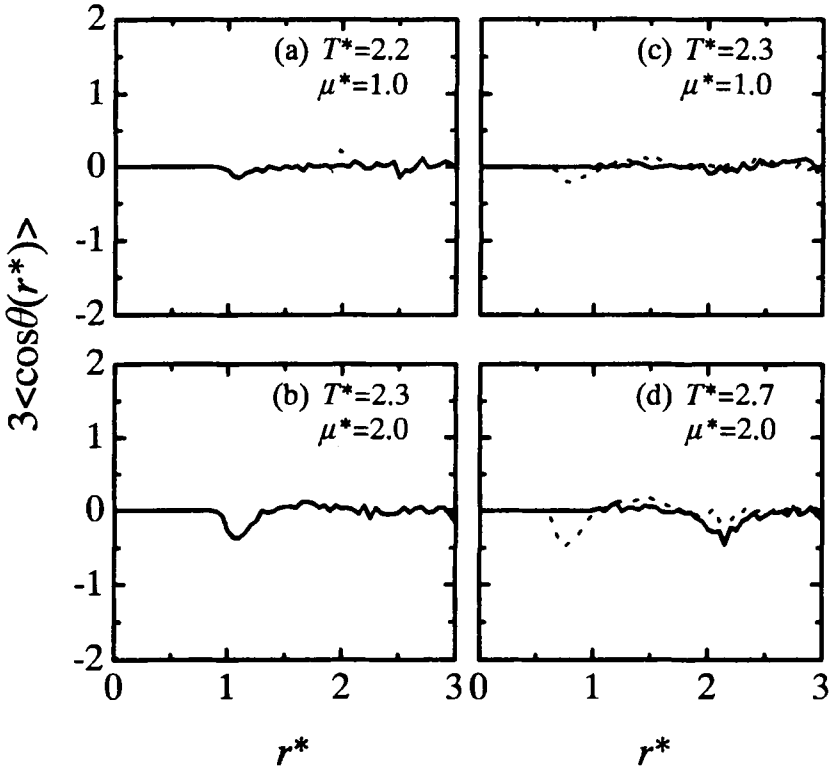

FIGURE 4 The dipole-dipole correlations as a function of intermolecular distance in the nematic phase at $\langle P_2 \rangle \approx 0.6$. Solid lines denote them as a function of separation between the centers-of-mass and dotted lines as a function of separation between the point dipoles. (a), (b) central dipolar systems; (c), (d) terminal dipolar systems.

$\langle P_2 \rangle$ for each μ^* value. For the terminal case (c), (d), the negative peak of the curve as a function of the separation between the point dipoles (dotted line) is positioned at *ca.*0.7 owing to the ellipsoidal shape. The peak indicates the formation of antiparallel dimers between layers. On the other hand, the first positive peak at *ca.*1.1 of the curve as a function of the center-of-mass (solid line) for the system with $\mu^* = 2.0$ (d) indicates the parallel dimers in a layer, although the peak does not appear for the terminal dipolar system with $\mu^* = 1.0$ (c). The positive peak at *ca.*1.2 of the curves (c), (d) as a function of the separation between the point dipoles (dotted line) certainly represents a parallel dimer in a layer, and the negative peak at *ca.*1.9 indicates a sign of an antiparallel pair of the molecule in different layers.

Downloaded by [University of California, San Diego] at 22:02 20 August 2012

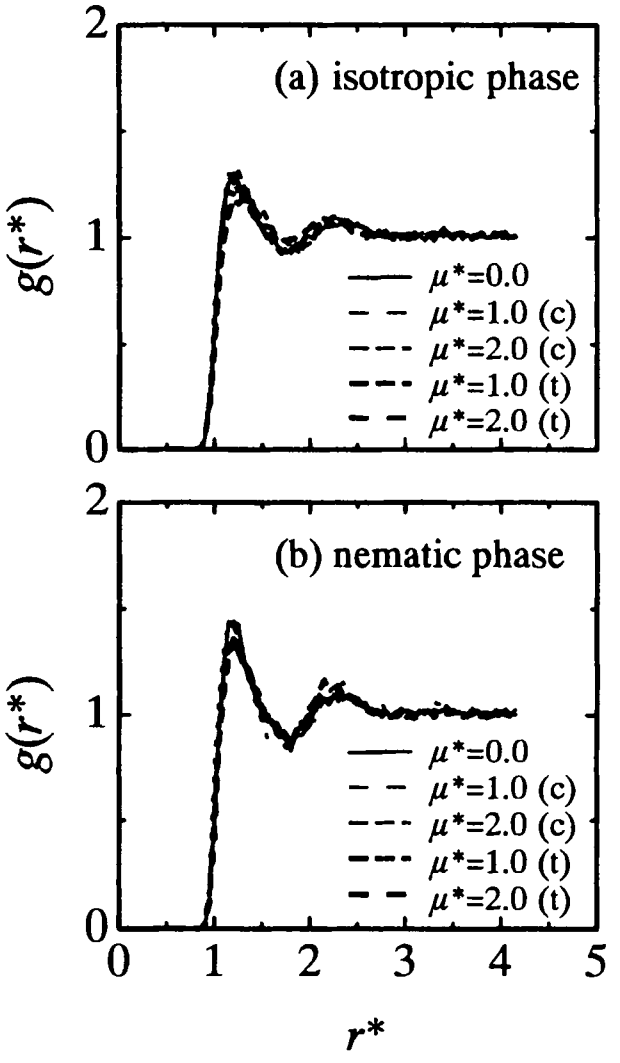

FIGURE 5 The center-of-mass radial distribution functions in the isotropic (a) and nematic (b) phase at $\langle P_2 \rangle \approx 0.6$. The symbols '*t*' and '*c*' represent the terminal and the central dipolar system, respectively.

Figure 8 shows the correlation functions for the central and the terminal dipolar systems in the crystalline phase whose assignment was done in the same manner as the smectic phase. The peaks are further enhanced in comparison with those in the smetic phase. The positive broad peak at *ca.*1.8–2.1 for the central dipolar system (a), (b) corresponds to parallel pairs

Downloaded by [University of California, San Diego] at 22:02 20 August 2012

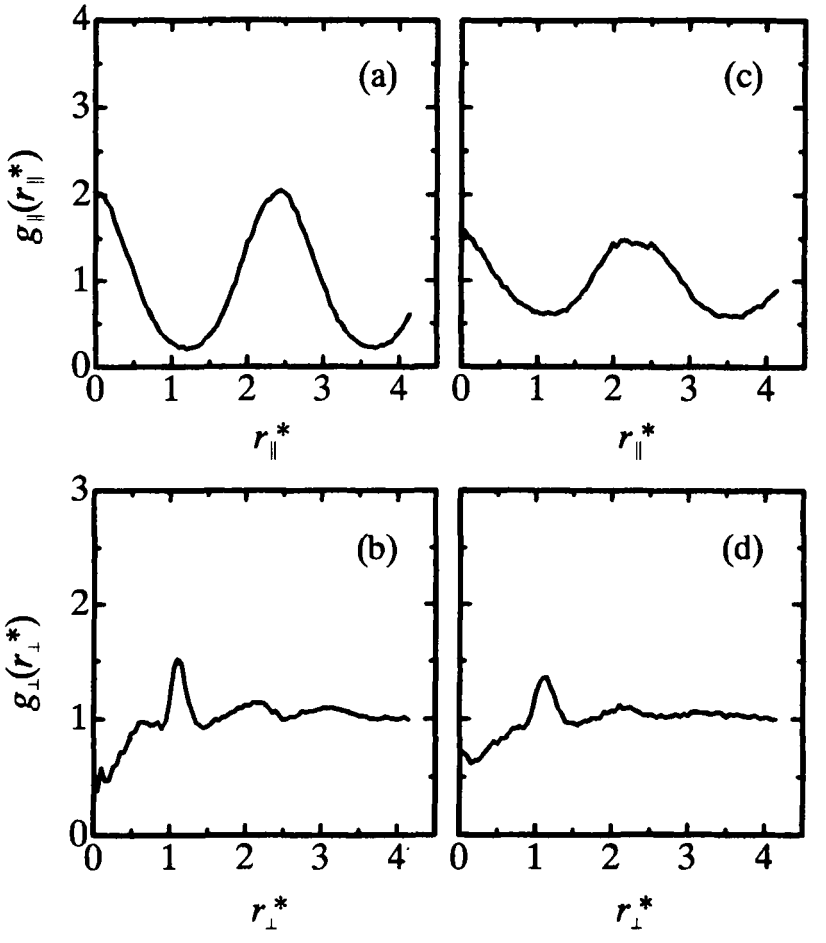

FIGURE 6 The longitudinal and transverse pair correlations as a function of intermolecular distance in the smectic phase for terminal dipolar systems with $\mu^* = 1.0$ (a), (b), 2.0 (c), (d).

in the second nearest neighbor in a layer. In the terminal system with $\mu^* = 2.0$ (d), the positive peak at *ca.*1.5 of the curve as a function of the separation between the center-of-mass (solid line) may indicate the formation of parallel arrangements in the interdigitated layers, and also the positive peak at *ca.*2.3 indicates parallel arrangements in the second nearest neighbor in a layer. However there is little correlation in this region for the system with $\mu^* = 1.0$ (c). Consequently, the layer structures and the dipolar correlation for the terminal dipolar systems are found to depend on the strength of the dipole.

Downloaded by [University of California, San Diego] at 22:02 20 August 2012

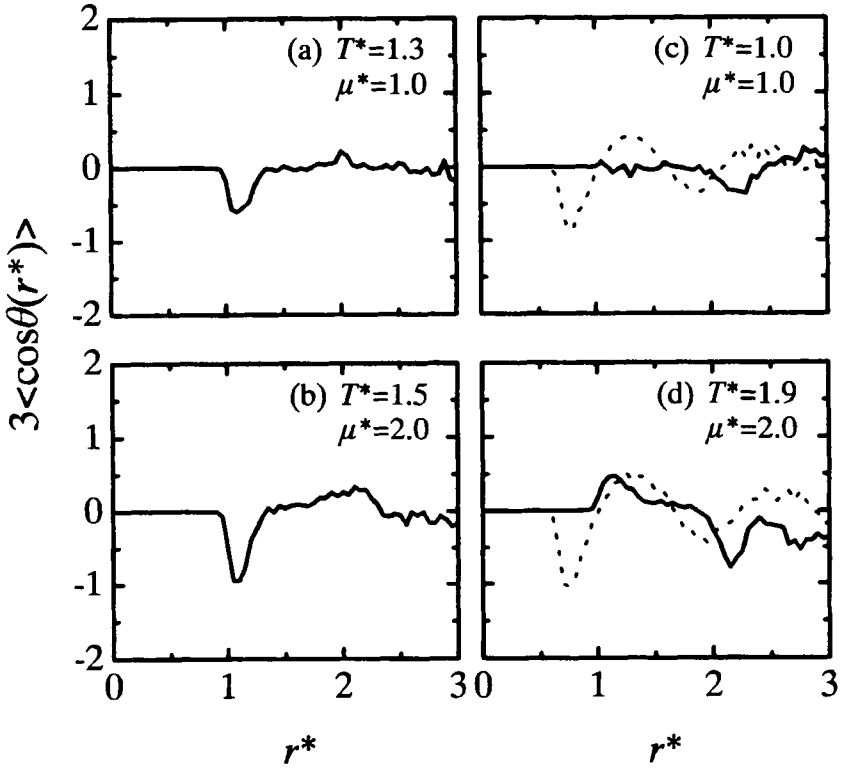

FIGURE 7 The dipole-dipole correlations as a function of intermolecular distance in the smectic phase with $\langle P_2 \rangle$ of *ca.*0.91 (a), (c) for $\mu^* = 1.0$ and *ca.*0.88 (b), (d) for $\mu^* = 2.0$. Solid lines denote them as a function of the separation between the centers-of-mass and dotted lines as a function of the separation between the point dipoles. (a), (b) central dipolar systems; (c), (d) terminal dipolar systems.

From considering the above results, the positional analysis within a layer is desired. Dipole direction, *i.e.* 'up' or 'down', within a layer must be tested to provide an essential feature for ferroelectric behavior. This will be confirmed by visualizing the distributions of the center-of-mass and also dipolar pointing, 'up' or 'down', for each particle. Figures 9 and 10 show the snapshots in the smectic and crystal phases confirmed by using the longitudinal and transverse pair correlations, respectively. In the smectic phase, the unpolarized phase is formed independent of the strength of the dipole. The picture shows the expected random arrangement of the particles, and also reveals that almost the same number of particles are in the opposite direction. This is quite natural behavior from the standpoint of energy. There is neither a positional order nor an order of dipole direction within a

Downloaded by [University of California, San Diego] at 22:02 20 August 2012

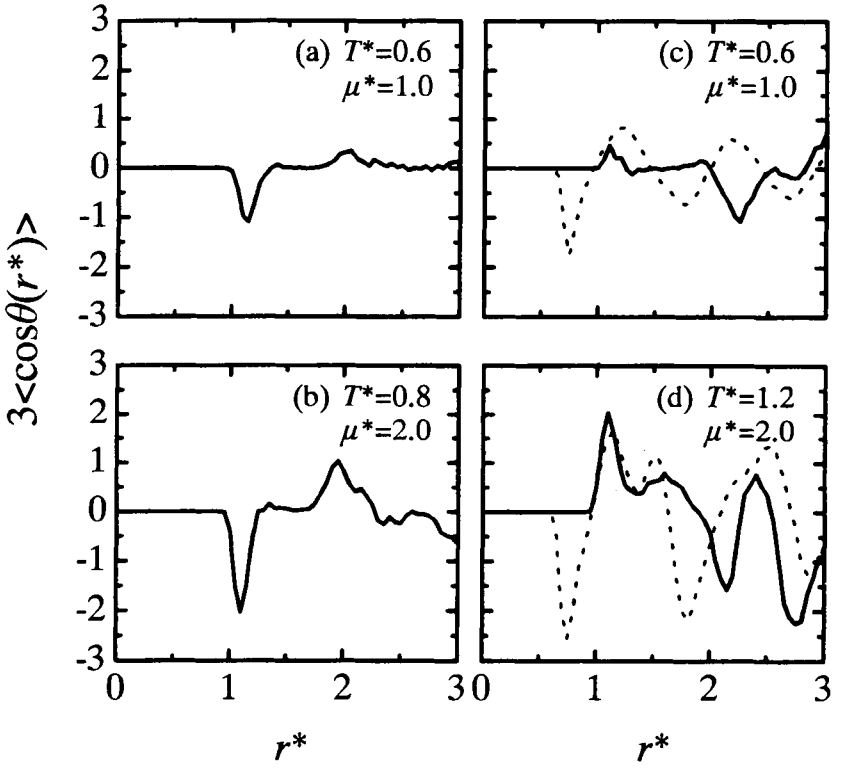

FIGURE 8 The dipole-dipole correlations as a function of intermolecular distance in the crystal phase with $\langle P_2 \rangle$ of *ca.*0.97 (a), (c) for $\mu^* = 1.0$ and *ca.*0.96 (b), (d) for $\mu^* = 2.0$. Solid lines denote them as a function of the separation between the centers-of-mass and dotted lines as a function of the separation between the point dipoles. (a), (b) central dipolar systems; (c), (d) terminal dipolar systems.

layer. Therefore, these phases shown in Figure 9 can be identified as the smectic A phase. In the crystal phase, the structure in a layer for the systems with $\mu^* = 0.0$ and 1.0 has undoubtedly a hexagonal symmetry though not quite perfect. On the other hand, the strong polar system with $\mu^* = 1.5$ or 2.0 forms not a hexagonal structure which is stable energetically but a tetragonal structure. The difference in structures formed accounts for the reason why the strong dipolar systems resist crystallization. Inspection of the snapshots shows that no polarization is observed within a layer as well as in the smectic phase on the whole [26]. Although dipole direction for the system with $\mu^* = 1.0$ is shown to be random, small clusters made up of molecules having the same direction of dipole are formed for the system with $\mu^* = 1.5$. It is found for the system with $\mu^* = 2.0$ that the larger clusters

Downloaded by [University of California, San Diego] at 22:02 20 August 2012

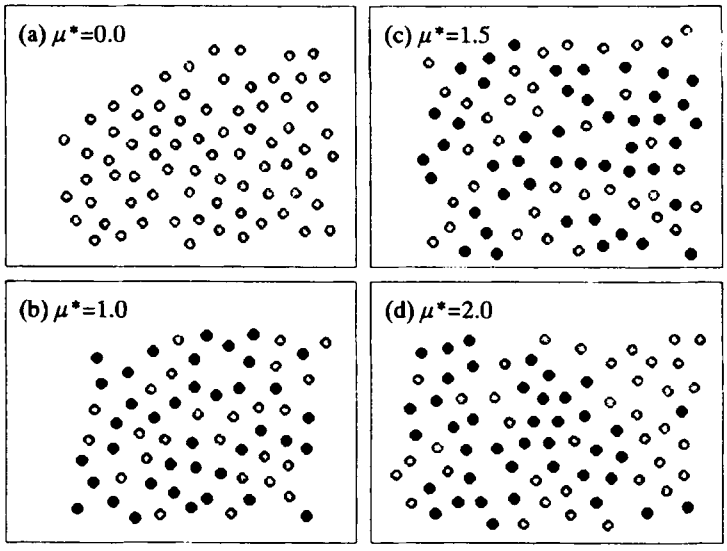

FIGURE 9 Snapshots of typical configurations within a layer in the smectic phase at $\langle P_2 \rangle$ of *ca.*0.88 for the systems with various μ^* values. (a) $\mu^* = 0.0$, (b) $\mu^* = 1.0$, (c) $\mu^* = 1.5$, (d) $\mu^* = 2.0$. The direction of dipole of 'up' or 'down' is distinguished by different colors.

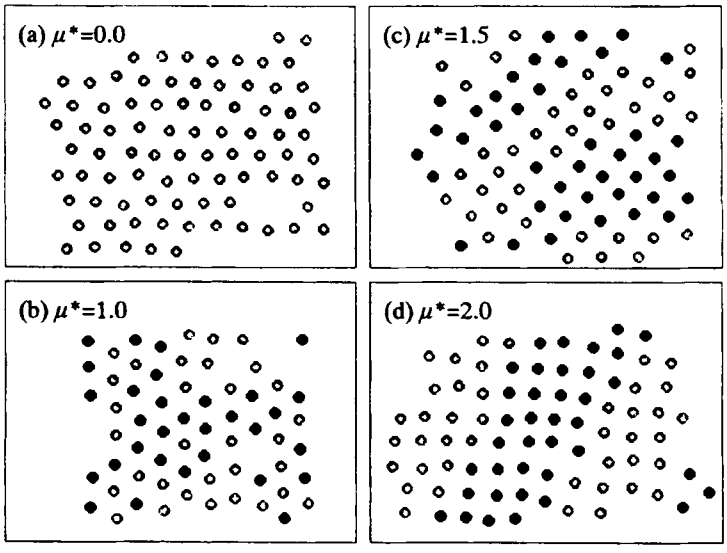

FIGURE 10 Snapshots of typical configurations within a layer in the crystal phase at $\langle P_2 \rangle$ of *ca.*0.97 for the systems with various μ^* values. (a) $\mu^* = 0.0$, (b) $\mu^* = 1.0$, (c) $\mu^* = 1.5$, (d) $\mu^* = 2.0$. The direction of dipole of 'up' or 'down' is distinguished by different colors.

Downloaded by [University of California, San Diego] at 22:02 20 August 2012

Downloaded by [University of California, San Diego] at 22:02 20 August 2012

are formed and the adjacent clusters are in the opposite direction, and also that clusters in the upper and lower layers are in the opposite direction alternately. Therefore, the clusters with various sizes depending on the dipolar strength forms in the system with the dipole located near the end of a molecule, and the dipoles are aligned parallel in a cluster. This result without any detectable formation of a ferro- or antiferroelectric smectic phase is reasonable on the analogy of the results in a system of dipolar hard spherocylinders [24].

In Figure 11, the density modulation which is the projection of the center-of-mass on a plane parallel to the director shows clearly the layer formation for the terminal dipolar system, together with the non-polar system as a reference. The number of the periodicity wave depends on the structure spontaneously formed from the initial isotropic configurations. Modulations as both functions of the center-of-mass and the point dipoles show similar behavior in the case of $\mu^* = 1.0$ regardless of the different $\langle P_2 \rangle$ value. In the case of $\mu^* = 2.0$, no difference are found in the modulations in the smectic phase ($T^* = 1.7$), although there are difference in the modulations in the crystal phase ($T^* = 1.2$). In order to evaluate the effect of dipolar position on layer formation the density modulations are shown for the dipolar systems with $\langle P_2 \rangle$ of *ca.*0.96 for $\mu^* = 0.0$ and 2.0 in Figure 12. The apparent difference in the sharpness of the density waves can be found in the systems. The sharpness in the density modulations for the central dipolar system is similar to that in the distribution denoted by the dotted line as a function of the separation between the point dipoles for the terminal system. The positional order of the dipole is higher than that of the center-of-mass for the terminal dipolar system. This was also clearly shown in the longitudinal pair correlation [26]. Therefore, the position of the dipole influences the layer formation. However the positional order is not sensitive to the dipolar strength in the smectic phase.

4. CONCLUSIONS

Monte Carlo simulations of the Gay-Berne molecules with the dipole located near the end of a molecule have been performed using the reaction field in a treatment of long-range dipolar interaction. The temperature dependence of the orientational and positional order in various phases has been studied at a fixed number density.

It is found that a short-range orientational order appears from the formation of antiparallel pairs not only in the nematic phase but also even in the

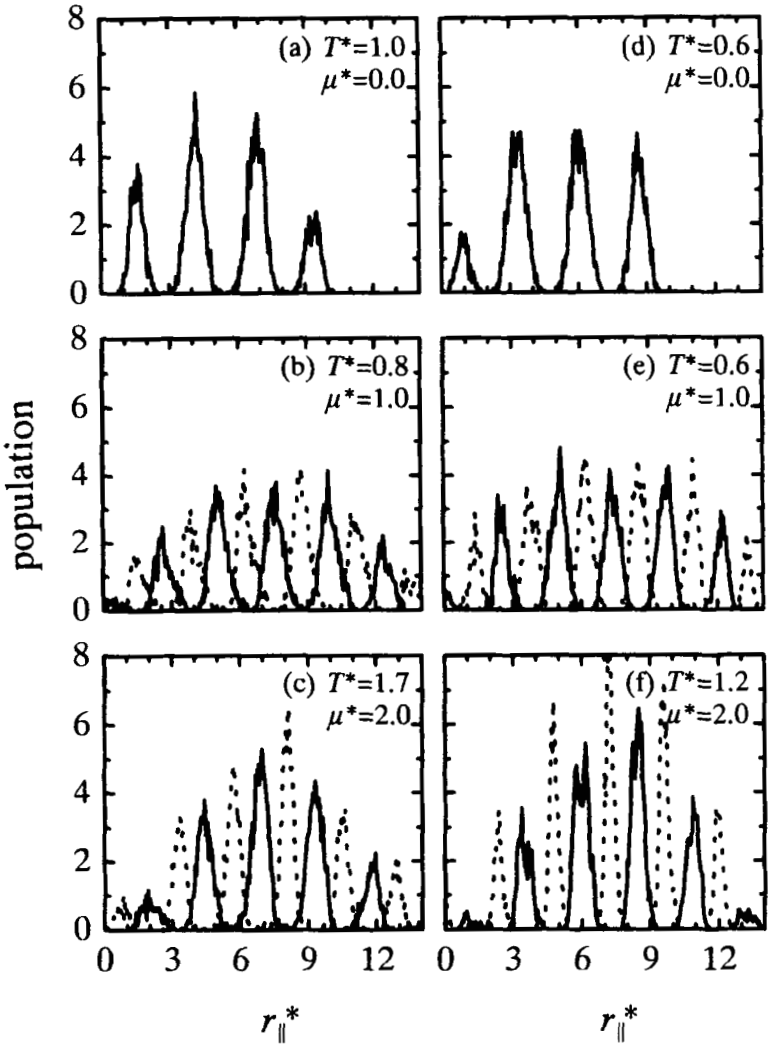

FIGURE 11 The density modulation with $\langle P_2 \rangle$ of *ca.*0.94 (a), (b), (c) and *ca.*0.97 (d), (e), (f). (a), (d) non-polar systems (b), (e) central dipolar systems; (c), (f) terminal dipolar systems. Solid curve denotes the modulation as a function of the separation between the centers-of-mass and dotted curve denotes the modulations as a function of the separation between the point dipoles.

isotropic phase. In the smectic phase, the distributions as a function of the separation between the point dipoles are sharper than those of the centers-of-mass as the dipole moment is increased. Interdigitated layers are found to be formed in which the molecules are mainly aligned in antiparallel

Downloaded by [University of California, San Diego] at 22:02 20 August 2012

Downloaded by [University of California, San Diego] at 22:02 20 August 2012

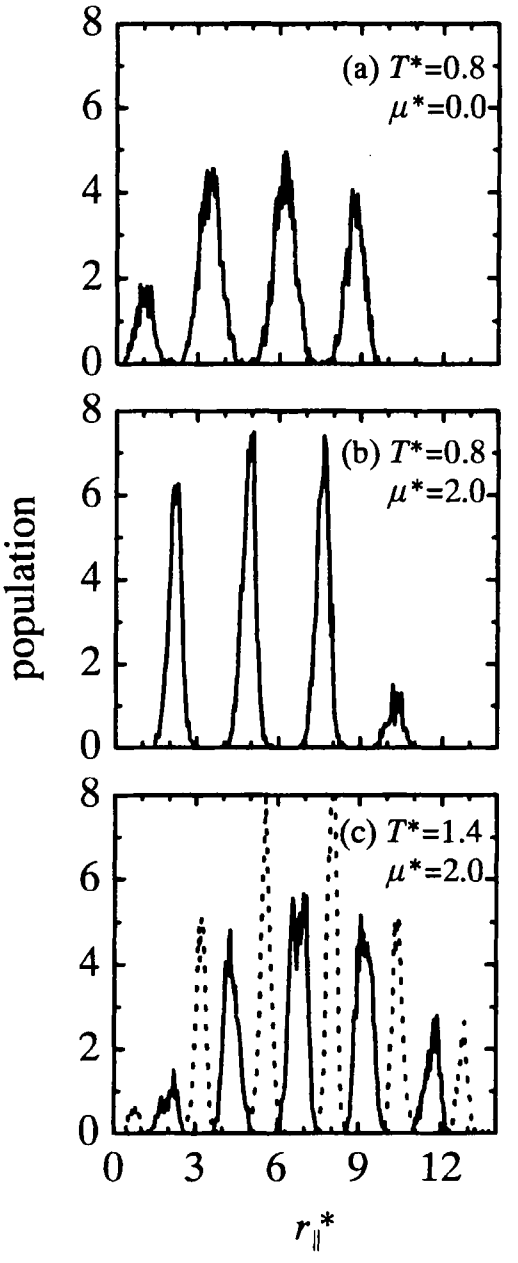

FIGURE 12 The density modulations with $\langle P_2 \rangle$ of *ca.*0.96. (a) non-polar systems; (b) central dipolar systems; (c) terminal dipolar systems. Solid curve denotes the modulation as a function of the separation between the centers-of-mass and dotted curve denotes the modulation as a function of the separation between the point dipoles.

relationship. From the analysis in a layer, the systems without polar and with $\mu^* = 1.0$ are found to form a hexagonal structure, and the strong polar systems with $\mu^* = 1.5$ and 2.0 form a tetragonal structure. Therefore, the strong dipole located near the end of a molecule disturbs the hexagonal structure which is energetically favorable. Furthermore, the strong dipolar molecules are found to form the clusters in which the molecules are aligned parallel in the crystal phase, and then the terminal dipoles contribute to decreasing layer spacing as the dipole is increased.

The simulations using the dipolar Gay-Berne model are capable of explaining the realistic behavior of a liquid crystal molecule containing a polar group such as cyano or nitro substituents, suggesting that this model is likely to be a useful tool for analyzing conventional polar liquid crystals.

Downloaded by [University of California, San Diego] at 22:02 20 August 2012

References

[1] M. P. Allen, G. T. Evans, D. Frenkel and M. Mulder, in *Advances in Chemical Physics*, Vol. LXXXVI, ed. I. Prigogine and S. A. Rice (John Wiley and Sons, Inc. 1993), p-1 and references therein.
[2] S. J. Picken, W. F. van Gunsteren, P. Th. van Duijnen and W. H. de Jeu, *Liq. Cryst.*, **6**, 357 (1989).
[3] M. R. Wilson and M. P. Allen, *Mol. Cryst. Liq. Cryst.*, **198**, 465 (1991).
[4] M. Yoneya and Y. Iwakabe, *Liq. Cryst.*, **18**, 45 (1995); *Langmuir*, **11**, 3516 (1995); *Liq. Cryst.*, **21**, 347 (1995).
[5] H. Toriumi, M. Yoshida, M. Mikami, M. Takeuchi and A. Mochizuki, *J. Phys. Chem.*, **100**, 15207 (1996).
[6] J. Vieillard-Baron, *Mol. Phys.*, **28**, 809 (1974).
[7] A. W. Stroobants, H. N. Lekkerkerker and D. Frenkel, *Phys. Rev. A*, **36**, 2929 (1987).
[8] D. Frenkel, B. M. Mulder and J. P. McTague, *Mol. Cryst. Liq. Cryst.*, **123**, 119 (1985).
[9] K. M. Aoki and F. Yonezawa, *Phys. Rev. A*, **46**, 59 (1992); *Phys. Rev. E*, **48**, 2025 (1993); K. M. Aoki and T. Akiyama, *Mol. Cryst. Liq. Cryst.*, **262**, 543 (1995); *Mol. Sim.*, **16**, 99 (1996).
[10] P. A. Lebwhol and G. Lasher, *Phys. Rev. A*, **6**, 426 (1972).
[11] G. R. Luckhurst and P. Simpson, *Mol. Phys.*, **47**, 251 (1982).
[12] J. G. Gay and B. J. Berne, *J. Chem. Phys.*, **74**, 3316 (1981).
[13] D. J. Adams, G. R. Luckhurst and R. W. Phippen, *Mol. Phys.*, **61**, 1575 (1987); E. de Miguel, L. F. Rull, M. K. Chalam and K. E. Gubbins, *Mol. Phys.*, **71**, 1223 (1990); E. de Miguel, L. F. Rull, M. K. Chalam, K. E. Gubbins and F. V. Swol, *Mol. Phys.*, **72**, 593 (1991).
[14] G. R. Luckhurst, R. A. Stephens and R. W. Phippen, *Liq. Cryst.*, **8**, 451 (1990).
[15] R. Berardi, A. P. J. Emerson and C. Zannoni, *J. Chem. Soc. Faraday Trans.*, **89**, 4069 (1993).
[16] A. P. J. Emerson, G. R. Luckhurst and S. G. Whatling, *Mol. Phys.*, **82**, 113 (1994).
[17] N. V. Madhusudana and J. Rajan, *Liq. Cryst.*, **7**, 31 (1990).
[18] S. Chandrasekhar, *Mol. Cryst. Liq. Cryst.*, **124**, 1 (1985).
[19] P. E. Cladis, in *Proceedings of the International Conference on Liquid Crystals, Bangalore*, 1970, ed. S. Chandrasekhar (Heyden, London), p. 105 (1980).
[20] L. Lei, *Mol. Cryst. Liq. Cryst.*, **144**, 41 (1987); K. M. Leung and L. Lei, *Mol. Cryst. Liq. Cryst.*, **144**, 71 (1987).
[21] J. Lee and S.-D. Lee, *Mol. Cryst. Liq. Cryst.*, **254**, 395 (1994).
[22] G. J. Zarragoicoechea, D. Levesque and J. J. Weis, *Mol. Phys.*, **75**, 989 (1992); G. J. Zarragoicoechea, D. Levesque and J. J. Weis, *Mol. Phys.*, **74**, 629 (1991).

[23] J. J. Weis, D. Levesque and G. J. Zarragoicoechea, *Phys. Rev. Lett.*, **69**, 913 (1992).
[24] D. Levesque, J. J. Weis and G. J. Zarragoicoechea, *Phys. Rev. E*, **47**, 496 (1993).
[25] K. Satoh, S. Mita and S. Kondo, *Liq. Cryst.*, **20**, 757 (1996).
[26] K. Satoh, S. Mita and S. Kondo, *Chem. Phys. Lett.*, **255**, 99 (1996).
[27] B. J. Berne and P. Pechukas, *J. Chem. Phys.*, **56**, 4213 (1972).
[28] J. Kushick and B. J. Berne, *J. Chem. Phys.*, **64**, 1362 (1976).
[29] N. Metropolis, A. W. Rosenbluth, M. N. Rosenbluth, A. H. Teller and E. Teller, *J. Chem. Phys.*, **21**, 1087 (1953).
[30] M. Neumann, *Mol. Phys.*, **50**, 841 (1983).
[31] C. G. Gray, Y. S. Sainger, C. G. Joslin, P. T. Cummings and S. Goldman, *J. Chem. Phys.*, **85**, 1502 (1986).
[32] C. Zannoni, in *The Molecular Physics of Liquid Crystals*, ed. G. R. Luckhurst and G. W. Gray (Academic Press, New York, London, 1979) chap 3.
[33] M. P. Allen and D. J. Tildesley, in *Comptuer Simulation of Liquids* (Clarendon Press, Oxford, 1989).
[34] D. Demus, H. Demus and H. Zaschke, in *Flüssige Kristalle in Tabellen* (VEB Deutscher Verlag für Grundstoff Industrie, Leipzig, 1974).
[35] D. Demus and H. Zaschke, in *Flüssige Kristalle in Tabellen II* (VEB Deutscher Verlag für Grundstoff Industrie, Leipzig, 1984).

Downloaded by [University of California, San Diego] at 22:02 20 August 2012